CARBON 49 (2011) 3356–3361

available at www.sciencedirect.com

ScienceDirect

journal homepage: www.elsevier.com/locate/carbon

Atomic chemisorption on graphene with Stone–Thrower–Wales defects

L. Chen [a,b,*], H. Hu [b], Yu. Ouyang [a], H.Z. Pan [a], Y.Y. Sun [a], F. Liu [b]

[a] Department of Physics, Linyi University, Linyi, Shandong 276005, People's Republic of China
[b] Department of Materials Science and Engineering, University of Utah, Salt Lake City, UT 84112, USA

ARTICLE INFO

Article history:
Received 17 February 2011
Accepted 13 April 2011
Available online 20 April 2011

ABSTRACT

Using first-principles calculations, we investigate the chemisorption of H, N, and P atoms on a graphene substrate with or without Stone–Thrower–Wales (STW) defects. Energetically, all three atoms are preferred to adsorb onto the defect sites by an energy difference of ~0.683–2.143 eV. In both the intrinsic and defected graphene, H atom adsorbs on top of a C atom, while N and P atoms adsorb at the bridge site between two C atoms with the N atom breaking the underneath C–C bond in the STW defect. Changes of atomic, electronic and magnetic structures associated with the atomic chemisorption on STW defects in graphene are discussed.

1. Introduction

Atomic chemisorption on graphene is expected to affect the fundamental properties of graphene, and conversely can be used as an effective mean to tailor the properties of graphene for potential applications. Most studies to date have focused on atomic chemisorption on intrinsic graphene. However, graphene, like all materials, contains defects [1,2] and therefore a study of atomic chemisorption on defective graphene is of both fundamental and practical interest.

Among many possible choices of adsorbates, H is one of the most studied atomic adsorbates on graphene by both theory and experiment. Hydrogen chemisorption on graphene has been shown to induce magnetism [3,4], to open band gap [5] in graphene and to drive formation of carbon nanotubes from graphene nanoribbons [6]. Another interesting class of adsorbates are so-called charge defects (or impurities), such as group V elements which have one extra valence electron than C atom. The chemisorption of charge defects on graphene is expected to induce large charge transfer and doping effect in graphene, which has been shown to affect the electron transport [7] and magnetic properties [8] of graphene. Therefore, we have chosen H and two group V elements N and P as examples for our study. We note that although N and P have similar chemical properties (in particular as charge defects), their atomic size is different, which may lead to different atomic configurations of chemisorptions and hence different effects on graphene electronic and magnetic properties as we show here.

On the other hand, a common type of defect in graphene, as in carbon nanotubes, is Stone–Thrower–Wales (STW) defect [9–15]. It is typically formed by a simple rotation of one C–C bond by 90° and consists of pairs of 5- and 7-atom rings. Rather than being a simple in-plane transformation of two carbon atoms, out-of-plane wavelike defect structures that extend over several nanometers are predicted [15]. STW defects have also been predicted to alter band structure and density of states of graphene, and hence to impact upon its transport properties [16–20]. Recent calculations show that such ring defects in graphene also modify graphene's chemical reactivity on chemisorption processes [21–23]. In particular, the presence of the defects has a strong influence on

* *Corresponding author at:* Department of Physics, Linyi University, Linyi, Shandong 276005, People's Republic of China. Fax: +86 05398766230.
E-mail address: Lchen.lyu@gmail.com (L. Chen).
0008-6223/$ - see front matter
doi:10.1016/j.carbon.2011.04.043

hydrogen chemical reactivity, shifting the chemisorption energy from highly unfavorable in the intrinsic graphene case to virtually energy neutral over a STW defect in curved graphene [19]. Overall, however, our understanding of chemisorptions on STW defects is still rather limited, which has motivated the present study.

We have carried out a comparative study to investigate H, N and P atom chemisorptions on the STW defected graphene versus the case of their chemisorptions on intrinsic graphene. We found that all three atoms are preferred to adsorb onto the defect sites. In both intrinsic and defective graphene, H atom adsorbs on top of a C atom, while N and P atoms adsorb at the bridge site between two C atoms with the N atom breaking the underneath C–C bond in the STW defect. The electronic structures including spin polarization are also analyzed for the two chemisorption cases for comparison.

2. Methods and parameters

Our calculations were performed using the pseudopotential plane-wave method within the spin-polarized generalized gradient approximation implemented in the Vienna Ab initio Simulation Package (VASP) as used before [24]. We used supercells containing 98 C atoms in a 7×7 super structure plus a vacuum layer of 13.35 Å, with a theoretically determined lattice constant $a = 2.46$ Å. Three chemisorption sites, hollow (*H*), bridge (*B*) and top (*T*) site, were considered for the chemisorptions of H, N and P atoms in intrinsic graphene, as shown in Fig. 1(a). For the 7×7 supercell with a STW defect, we varied the top chemisorption sites for H from T1 to T7, as indicated in Fig. 1(b), and the bridge chemisorption sites for N and P from B1 to B7, as indicated in Fig. 1(c). A $4\times4\times1$ k-point mesh for Brillouin zone sampling and a plane-wave cutoff of 400 eV were used. The system was relaxed until the force on each atom is minimized to be less than 0.01 eV/Å.

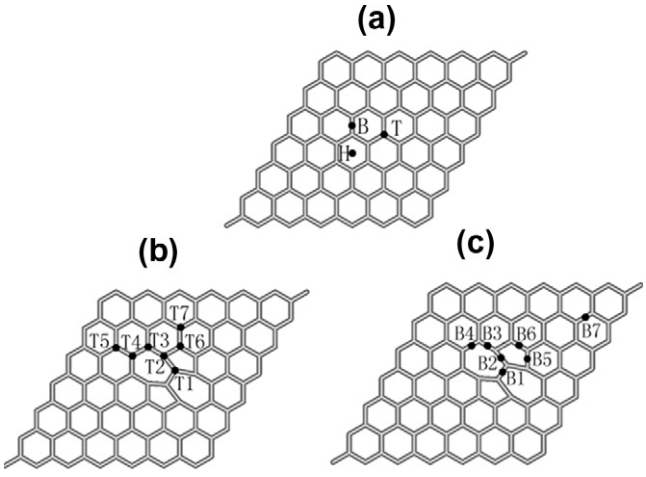

Fig. 1 – Illustration of chemisorption sites. (a) Three different chemisorption sites: the top, bridge, and hollow site in intrinsic graphene; (b) top site for H chemisorption on the STW defect; and (c) bridge site for N or P chemisorption on the STW defect.

3. Results and discussion

The chemisorption energies are calculated as $E_{ads} = E_{tot} - E_{graphene} - E_{atom}$, where E_{tot} and $E_{graphene}$ are the total energies of the graphene with and without adatoms respectively, and E_{atom} stands for the energy of a single adatom. From our calculation we found that energetically the most favorable chemisorption site is the top site for H with a chemisorption energy of −1.197 eV, and the bridge site for both N and P with a chemisorption energy of −2.85 and −0.728 eV, respectively, in agreement with the previous calculations [8,19,25]. In intrinsic graphene, each carbon atom is bonded with three neighboring carbon atoms in sp^2 hybridization, leaving one electron in the p_z orbital. For H chemisorption, the most stable configuration is for H atom to bond on top of a carbon atom forming an sp^3 hybrdization [6]. But for N or P chemisorption, however, N or P bonds vertically with two C atoms at the bridge site forming a planar, non-equivalent sp^2 hybridization [26] structure perpendicular to the graphene plane.

The presence of STW defect causes local changes of geometries in graphene. The rotated C–C bond length is compressed from 1.42 Å in intrinsic graphene to 1.32 Å, so that overall the STW defect induces a compressive strain to graphene. Because the in-plane graphene deformation is much stiffer than the out-of-plane deformation [27], in order to relax the compressive strain, the carbon atoms around the STW defect move out of plane [15]. The forming energy of single STW defect is calculated to be 5.1 eV per supercell. It is in agreement with the results by Ma et al. of 4–5 eV [15] considering the different long-range elastic defect–defect interactions for different supercell sizes. However, our focus here is the relative chemisorption energies on defect, so the exact formation energy of STW defect is not important.

The STW defect is expected to have a strong effect on the atomic chemisorption on graphene. Seven different top chemisorption sites T1–T7 as indicated in Fig. 1(b) for H were tested. We found that the most favored H chemisorption site is at T1, as shown in Fig. 2(a), where H is adsorbed on one of the C atoms in the "rotated" bond in agreement with the result of [19]. It's chemisorption energy is ~0.68 eV lower than that at the T5 site away from the STW defect, as shown in Table 1. For N chemisorption, seven different bridge sites B1–B7 as indicated in Fig. 1(c) were tested. We found that the most

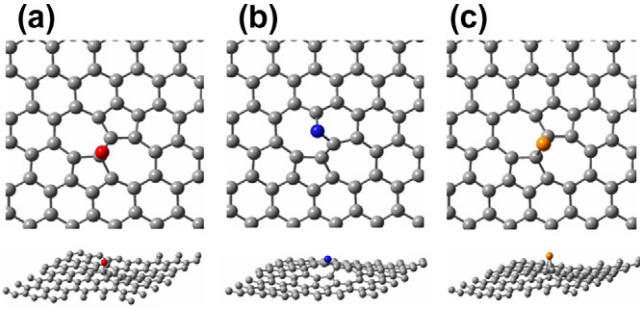

Fig. 2 – (a) The top (top panel) and side (bottom panel) view of the optimized structure of graphene with H chemisorption on the STW defect; (b) same as (a) with N chemisorption; (c) same as (a) with P chemisorption.

Table 1 – Relative chemisorption energies (see zero point of energy) in eV on the STW defected graphene at the top site for H chemisorption as shown in Fig. 1(b), and at the bridge site for N or P chemisorption as shown in Fig. 1 (c).

	Chemisorption on a STW defected graphene						
Sites	1	2	3	4	5	6	7
H	−0.683	−0.670	−0.242	−0.247	0.000	−0.422	−0.021
N	−1.089	−2.143	−1.714	−0.797	−0.712	−0.171	0.000
P	−1.181	–	−0.745	−0.395	−0.857	−0.374	0.000

favored chemisorption site is at B2, as shown in Fig. 2(b). It's chemisorption energy is ~2.14 eV lower than that at the B7 site outside of the STW defect, as shown in Table 1. The most favored chemisorption site for P is at B1 (Fig. 2(c)), where the chemisorption energy is ~1.18 eV lower than that at the B7 site (Table 1). These results show that the STW defect serves as a "trap" for atomic chemisorption; all three atoms, H, N and P are attracted to stay on the STW defect in graphene, energetically.

Fig. 3 shows a detailed comparison between the chemisorption structures (bond lengths and angles) of H, N and P on the intrinsic graphene (top panel) and those on the STW defects (bottom panel). On the intrinsic graphene, the distance between the absorbate and its neighboring carbon atoms at the stable chemisorption sites is shown in Table 2. The H-bonded C atom moves 0.39 Å outward away from the graphene plane, which breaks the symmetry of the graphene, and changes the sp^2 hybridization of the graphene to an sp^3 hybridization locally [6,19]. The N and P atoms, on the other hand, are bonded with two C atoms to form a stable configuration of non-equivalent sp^2 hybridization [26], forming a vertical triangular plane perpendicular to graphene plane. The two C atoms bonded to the N or P change to a sp^2–sp^3 hybridization, and move outward from the graphene plane by 1.10 and 0.50 Å for the case of N and P, respectively. The amplitude of graphene corrugation is smaller for P chemisorption, which indicates that the C–C bond below the P atom retains more of its sp^2 character and rehybridizes relatively weakly with the P atomic orbitals than the case of N. The equilibrium distance between the adatom and C is 1.13, 1.46 and 1.94 Å for H, N and P, respectively, as shown in the top panel of Fig. 3(a)–(c). The bond angle of C–N–C/C–P–C is 64.32°/45.58° and the C–C bond length below the N/P atom is 1.56 Å/1.51 Å. The bond length between the C atom bonded to the adatom and its neighboring C atoms is increased to 1.50, 1.46 and 1.46 Å from the original value of 1.42 Å, for H, N and P chemisorption, respectively.

For H chemisorption on the STW defect, the equilibrium H–C bond length is 1.11 Å, as shown in the bottom panel of Fig. 3(a), which is slightly shorter than 1.13 Å in the intrinsic graphene, as shown in the top panel of Fig. 3(a). The H–C–C angle with the two C atoms in the "rotated" bond is 109.75°, and the other H–C–C angle is 107.52°, indicating that the C atom bonded to H has an sp^3 hybridization in the STW defect, same as in the intrinsic graphene. The "rotated" C–C bond length is 1.43 Å, about the same as in the STW defect without H chemisorption.

For N chemisorption on the STW defect, the equilibrium N–C bond lengths are 1.39 Å (with the C atom in the "rotated" bond) and 1.33 Å (Fig. 3(b), bottom panel), which are less than 1.46 Å in the intrinsic graphene (Fig. 3(b), top panel). A notable structural feature is that N chemisorption breaks the C–C bond below, increasing distance of these two C atoms to 2.16 Å, which is different from the case of intrinsic graphene without breaking the C–C bond. The C–N–C angle is 104.99° (Fig. 3(b), bottom panel), showing an sp^3 hybridization, which is very different from 64.32° for N chemisorption on intrinsic graphene in an sp^2 hybridization without breaking the C–C

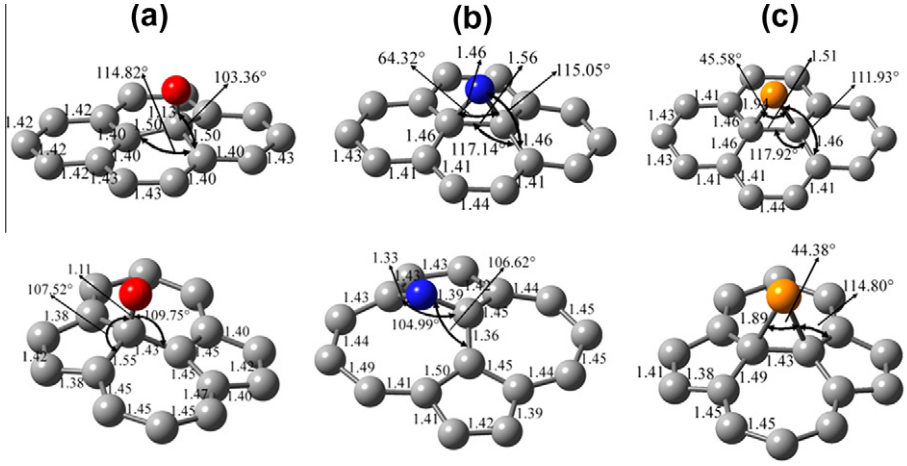

Fig. 3 – The bond lengths in Å and bond angles of different chemisorption species and structures. (a) H chemisorption; (b) N chemisorption and (c) P chemisorption. Top panel for the adatom on the intrinsic graphene and bottom panel on the STW defect in graphene.

Table 2 – The distances between the absorbed atom and its neighboring carbon atoms, $d_{c\text{-}atom}$, on intrinsic graphene at stable chemisorption sites. h denotes the maximum deviation (outward) of the C atoms relative to graphene plane, and μ stands for the total magnetic moment of the supercell.

	H(T)	N(B)	P(B)
$d_{c\text{-}atom}$ (Å)	1.13	1.46	1.94
h (Å)	0.39	1.10	0.50
μ (μ_B)	0.48	0.71	0.20

bond underneath N. The "rotated" C–C bond length is 1.36 Å, ~0.06 Å shorter than in the STW defect without N chemisorption.

For P chemisorption on the STW defect, the P atom bonds with the C atoms at a bridge site, in a non-equivalent sp^2 hybridization, similar to the case on intrinsic graphene. The equilibrium P–C bond length is 1.89 Å, slightly shorter than 1.94 Å in intrinsic graphene. The C–P–C angle is 44.39°, which is slightly smaller than 45.58° for P adsorption in intrinsic graphene. The "rotated" C–C bond is 1.43 Å (Fig. 3(c), bottom panel), which is about the same as the case on intrinsic graphene.

Next, we discuss and compare the electronic structures associated with the atomic chemisorption in the intrinsic and STW defected graphene. Fig. 4 shows the band structures (left panel) and spin density distributions (right panel) of H, N and P on the intrinsic graphene. For H chemisorption, two flat bands, spin up (red) and spin down (blue) appear around Fermi energy as shown in Fig. 4(a), indicating that the H chemisorption induces a localized state which is spin-polarized. Fig. 4(b) shows the isosurface of spin density (i.e. $\rho(\uparrow)-\rho(\downarrow)$). The spin polarization is induced on the C atoms around the chemisorption site and decay exponentially away from it. The total magnetic moment of the supercell is 0.48μ_B. It is very interesting to see that the magnetic ordering induced by H chemisorption in graphene (Fig. 4(b)) is very similar to that induced by a C vacancy [24,28,29] in graphene. This is because one consequence that H chemisorption has is to remove local π bands as it changes the C atom from sp^2 to sp^3 hybridization just as if this C atom were removed. In the pristine graphene, the π band, residing on the A-sublattice, are degenerate with the π^* band, residing on the B-sublattice, at Fermi energy. When H adsorbs onto a C atom of A (B) sublattice, it effectively creates B (A) zigzag edges, by breaking the π bonding between the adsorbed C and its three neighbors, which gives rise to flat bands of edge states at the Fermi energy (Fig. 4(a)), same as a vacancy will do. Consequently, the resulting magnetism is the same as the edge magnetism [24,28,29] produced by a vacancy. We note that it is well-known in graphene that only the π bands are present at and near Fermi level, while the σ bands are far away by 1–2 eV from the Fermi level. Thus, in most situations concerning ground-state or low excitation properties, only π bands need

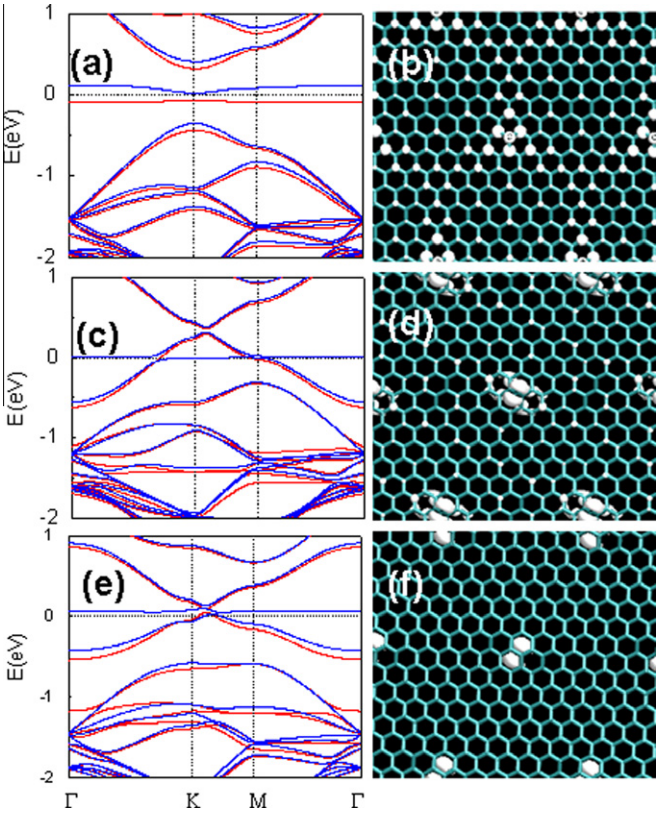

Fig. 4 – The spin-up (red) and spin-down (blue) band structures and the spin density distributions, with the spin density isosurface set to be 0.03 e/Å^3, for chemisorptions on the intrinsic graphene. (a) and (b) H chemisorption; (c) and (d) N chemisorption; (e) and (f) P chemisorption. Fermi energy is set as 0.0 eV. (For interpretation of the references to color in this figure legend, the reader is referred to the web version of this article.)

to be taken into account [30]. This is why when considering the spin polarization in π electrons at the zigzag edge, H chemisorption (without changing C–C σ bonds) and C vacancy (creating three σ dangling bonds) give rise to the same effect.

For N chemisorption on the graphene, Fermi energy shifts downward below the original Dirac point, as shown in Fig. 4(c). This indicates that there is certain amount of charge transfer from graphene to N, making the graphene slightly *p*-type doped. Because the bridging N atom bonds with two C atoms (one from the A sublattice and the other from the B sublattice), there is no N-induced magnetism in graphene (Fig. 4(d)), as the case of H chemisorption (Fig. 4(b)). However, the N atom itself is spin-polarized with a large moment of $0.84\mu_B$, which in turn slightly spin-polarizes its neighboring C atoms and induces small magnetic moments on them. The reason for N spin polarization can be understood from its bonding and electronic configuration. Nitrogen is in a non-equivalent sp^2 hybridization with two sp^2 orbitals forming N–C bonds and one sp^2 orbital occupied with an electron pair, which differs from the equivalent sp^2 hybridization with three identical sp^2 orbitals. Among five valence electrons of N, two form covalent bands with its neighboring C atoms, and two form a lone pair in the sp^2-like orbitals. This leaves one last electron in the p_z orbital, which is perpendicular to the local C–N–C (sp^2) plane, parallel to the graphene. This "unpaired" p_z electron is spin polarized, giving a large magnetic moment on N, as shown in Fig. 4(d).

For P chemisorption on the graphene, the band structure shown in Fig. 4(e) is similar with that of N chemisorption, except the Fermi energy lies almost at the Dirac point. This is possibly because the P–C bond is weaker than the N–C bonds, so that there is much less charge transfer between the P and C atoms than the N and C atoms. The magnetism induced by P chemisorption (Fig. 4(f)) shares the same mechanism with that of N chemisorption discussed above. The magnetic moment is $0.2\mu_B$, much smaller than that induced by N chemisorption, for the weak interaction between P and C atoms.

Fig. 5(a)–(c) shows the band structure of H, N and P chemisorption on the STW defect. Different from H chemisorption on the intrinsic graphene, the electronic structure of H chemisorption on the STW defect is not spin-polarized, showing a *p*-doped behavior. This is because the STW defect already breaks locally the A–B lattice symmetry in graphene and opens a gap for the π–π^* bands, so that H chemisorption would not induce the edge states as on the intrinsic graphene. For N chemisorption on the STW defect, it makes the system *p*-doped, same as the case of N chemisorption on intrinsic graphene, because of charge transfer from graphene to N. However, there is no magnetism, because N atom is no longer spin polarized in an sp^3 configuration (with N breaking the C–C bonds underneath) different from the case of intrinsic graphene in an sp^2 configuration. For the P chemisorption on the STW defect, the electronic structure is rather similar to the case of P chemisorption on the intrinsic graphene because the atomic chemisorption structure is similar in two cases. The ground state is spin polarized as shown in Fig. 5(c), as the P atom is spin-polarized in an sp^2 configuration with a magnetic moment of $0.2\mu_B$, which in turn induces small spin density in its neighboring C atoms, as shown in Fig. 5(d). The charge distributions in Fig. 5(e)–(f) reflect the bonding properties for N and P atom chemisorption on STW defected graphene, respectively. It clearly shows there is a charge transfer from graphene to P and N, indicating the *p*-doped graphene, and also there is much less charge transfer from graphene to P than to N.

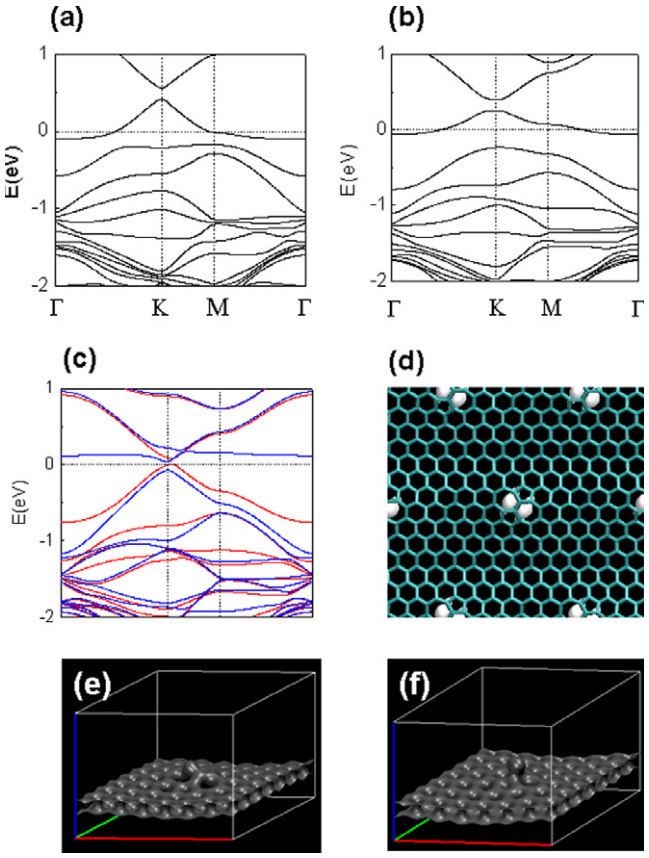

Fig. 5 – (a) The band structure of the chemisorption structure in Fig. 2(a); (b) the band structure of the chemisorption structure in Fig. 2(b); (c) the band structure of the chemisorption structure in Fig. 2(c). All labels are the same as in Fig. 4(a). (d) The spin density distributions of the chemisorption structure in Fig. 2(c); the spin density isosurface is set to be 0.03 e/Å^3. The charge density distribution with the charge density isosurface at 0.50 eÅ^3 (e) for N adsorbed graphene; (f) for P adsorbed graphene.

4. Conclusions

We have performed a comparative study and analyzed in detail the atomic and electronic structures associated with the H, N and P chemisorption on intrinsic graphene versus the case on the STW defected graphene. For H chemisorption, the atomic structure is similar in the two cases with H at the top site, but the electronic structure differs dramatically. The H induces spin polarization in the intrinsic graphene but not in the STW defected graphene, because the STW defect already breaks locally the A–B lattice symmetry. For N chemisorption, the atomic structure is very different in the two cases even though N is at the bridge site at both cases. Nitrogen breaks the underneath C–C bond in the STW defected

graphene but not in the intrinsic graphene. Consequently, the electronic structure is also very different: N is in an sp^2 hybridization on the intrinsic graphene with magnetism but in an sp^3 hybridization on the STW defect without magnetism. For P chemisorption, both the atomic and electronic structure is similar in the two cases, with P at the bridge site in an sp^2 hybridization with small magnetism.

Acknowledgments

The authors wish to express their deep thanks to Dr. Xiuwen Zheng and Dongjiao Li for their helpful discussions. The work is supported by the National Natural Science Foundation in China Grant No. 10974076. The work at Utah was supported by DOE-BES program (Grant DE-FG02-04ER46148 & DE-FG02-03ER46027). First-principles calculations are performed on computers at CHPC of Utah and Linyi University in China.

REFERENCES

[1] Hashimoto A, Suenaga K, Gloter A, Urita K, Iijima S. Direct evidence for atomic defects in graphene layers. Nature 2004;430:870–3.
[2] Huang B, Liu F, Wu J, Gu BL, Duan WH. Suppression of spin polarization in graphene nanoribbons by edge defects and impurities. Phys Rev B 2008;77:153411(1)–4).
[3] Soriano D, Muñoz-Rojas F, Fernández-Rossier J, Palacios JJ. Hydrogenated graphene nanoribbons for spintronics. Phys Rev B 2010;81:165409(1)–7).
[4] Li WF, Zhao MW, He T, Song C, Lin XH, Liu XD, et al. Concentration dependent magnetism induced by hydrogen adsorption on graphene and single walled carbon nanotubes. J Magn Magn Mater 2010;322:838–43.
[5] Berashevich J, Chakraborty T. Tunable band gap and magnetic ordering by adsorption of molecules on graphene. Phys Rev B 2009;80:033404(1)–33404(4).
[6] Yu D, Liu F. Synthesis of carbon nanotubes by rolling up patterned graphene nanoribbons using selective atomic adsorption. Nano Lett 2007;7:3046–50;
Wang ZF, Zhang Y, Liu F. Formation of hydrogenated graphene nanoripples by strain engineering and directed surface self-assembly. Phys Rev B 2011;83. 041403(R)(1)-4).
[7] Yan Q, Huang B, Yu J, Zheng F, Zang J, Wu J, et al. Intrinsic current–voltage characteristics of graphene nanoribbon transistors and effect of edge doping. Nano Lett 2007;7:1469–73.
[8] Wu M, Liu EZ, Jiang JZ. Magnetic behavior of graphene absorbed with N, O and F atoms: a first-principles study. Appl Phys Lett 2008;93:08250(1)–8250(3).
[9] Thrower PA. The study of defects in graphite by transmission electron microscopy. In: Walker PL, editor. Chemistry and physics of carbon. New York: Marcel Dekker; 1969. p. 217.
[10] Stone A, Wales DJ. Theoretical studies of icosahedral C60 and some related species. Chem Phys Lett 1986;128:501–3.
[11] Ewels CP, Heggie MI, Briddon PR. Adatoms and nanoengineering of carbon. Chem Phys Lett 2002;351:178–82.
[12] Buongiorno-Nardelli M, Yakobson BI, Bernholc J. Brittle and ductile behavior in carbon nanotubes. Phys Rev Lett 1998;81:4656–9.
[13] Buongiorno-Nardelli M, Yakobson BI, Bernholc J. Mechanism of strain release in carbon nanotubes. Phys Rev B 1998;57:R4277–80.
[14] Samsonidze GG, Samsonidze GG, Yakobson BI. Kinetic theory of symmetry-dependent strength in carbon nanotubes. Phys Rev Lett 2002;88:065501(1)–65501(4).
[15] Ma J, Alfè D, Michaelides A, Wang EG. Stone–Wales defects in graphene and other planar sp^2-bonded materials. Phys Rev B 2009;80:033407(1)–33407(3).
[16] Kang J, Bang J, Ryu B, Chang KJ. Effect of atomic-scale defects on the low-energy electronic structure of graphene: perturbation theory and local-density-functional calculations. Phys Rev B 2008;77:115453(1)–9).
[17] Carlsson JM, Scheffler M. Structural electronic and chemical properties of nanoporous carbon. Phys Rev Lett 2006;96:046806(1)–46806(4).
[18] Boukhvalov DW, Katsnelson MI. Chemical functionalization of graphene with defects. Nano Lett 2008;8:4373–9.
[19] Duplock EJ, Scheffler M, Lindan PJD. Hallmark of perfect graphene. Phys Rev Lett 2004;92:225502(1)–4).
[20] Huang B, Liu M, Su NH, Wu J, Duan WH, Gu BL, et al. Quantum manifestations of graphene edge stress and edge instability: a first-principles study. Phys Rev Lett 2009;102:166404(1)–4).
[21] Letardi S, Celino M, Cleri F, Rosato V. Atomic hydrogen adsorption on a Stone–Wales defect in graphite. Surf Sci 2002;496:33–8.
[22] Arellano JS, Molina LM, Rubio A, López MJ, Alonso JA. Interaction of molecular and atomic hydrogen with (5, 5) and (6, 6) single-wall carbon nanotubes. J Chem Phys 2002;117:2281–8.
[23] Zhou LG, Shi SQ. Adsorption of foreign atoms on Stone–Wales defects in carbon nanotube. Carbon 2003;41:613–25.
[24] Chen L, Yu DC, Liu F. Magnetism in nanopatterned graphite film. Appl Phys Lett 2008;93:223106(1)–3).
[25] Zhou YG, Zu XT, Gao F, Lv HF, Xiao HY. Adsorption-induced magnetic properties and metallic behavior of graphene. Appl Phys Lett 2009;95:123119(1)–3).
[26] Zhou XT, Sham TK, Wu Y, Chong YM, Bello I, Lee ST, et al. X-ray excited optical luminescence from diamond thin films: the contribution of sp2- and H-bonded carbon to the luminescence. J Am Chem Soc. 2007;129:1476–7.
[27] Sun DY, Shu DJ, Ji M, Liu F, Wang M, Gong XG. Pressure-induced hard-to-soft transition of a single carbon nanotube. Phys Rev B 2004;70:165417(1)–5).
[28] Yu D, Lupton EM, Liu M, Liu W, Liu F. Collective magnetic behavior of graphene nanohole superlattices. Nano Res 2008;1:56–62.
[29] Yu D, Lupton EM, Gao HJ, Zhang C, Liu F. A unified geometric rule for designing nanomagnetism in graphene. Nano Res 2008;1:497–501.
[30] Wang ZF, Liu F. Manipulation of electron beam propagation by hetero-dimensional graphene junctions. ACS Nano 2010;4:2459.